Nature of the polaron-molecule transition in Fermi polarons

Cheng Peng,[1,2,*] Ruijin Liu,[1,*] Wei Zhang,[3,4] and Xiaoling Cui[1,5,†]

[1]*Beijing National Laboratory for Condensed Matter Physics, Institute of Physics, Chinese Academy of Sciences, Beijing 100190, China*

[2]*School of Physical Sciences, University of Chinese Academy of Sciences, Beijing 100049, China*

[3]*Department of Physics, Renmin University of China, Beijing 100872, China*

[4]*Beijing Key Laboratory of Opto-electronic Functional Materials and Micro-nano Devices, Renmin University of China, Beijing 100872, China*

[5]*Songshan Lake Materials Laboratory, Dongguan, Guangdong 523808, China*

(Received 3 March 2021; revised 1 June 2021; accepted 7 June 2021; published 21 June 2021)

It has been commonly believed that a polaron-to-molecule transition occurs in three-dimensional (3D) and 2D Fermi polaron systems as the attraction between the single impurity and majority fermions gets stronger. The conclusion has been drawn from the separate treatment of polaron and molecule states and thus deserves a close reexamination. In this work, we explore the physics of polarons and molecules by utilizing a unified variational *Ansatz* with up to two particle-hole (ph) excitations (V-2ph). We confirm the existence of a first-order transition in 3D and 2D Fermi polarons, and we show that the nature of such a transition lies in an energy competition between systems with different momenta, $\mathbf{Q} = \mathbf{0}$ and $|\mathbf{Q}| = k_F$; here $\mathbf{Q}$ is defined as the momentum of a Fermi polaron system with respect to the Fermi sea of majority fermions (with Fermi momentum k_F). The literally proposed molecule *Ansatz* is identified as an asymptotic limit of the $|\mathbf{Q}| = k_F$ state in a strong-coupling regime, which implies a huge SO(3) (for 3D) or SO(2) (for 2D) ground-state degeneracy in this regime. The recognition of such degeneracy is crucially important for evaluating the molecule occupation in realistic systems with finite impurity density and at finite temperature. To compare with recent experiment of 3D Fermi polarons, we have calculated various physical quantities under the V-2ph framework, and we obtained results that are in good agreement with experimental data in the weak-coupling and near-resonance regime. Further, to check the validity of our conclusion in 2D, we have adopted a different variational method based on the Gaussian sample of high-order ph excitations (V-Gph), and we found the same conclusion on the nature of the polaron-molecule transition therein. For a 1D system, the V-2ph method predicts no sharp transition, and the ground state is always at the $\mathbf{Q} = \mathbf{0}$ sector, consistent with the exact Bethe-*Ansatz* solution. The presence/absence of a polaron-molecule transition is analyzed to be closely related to the interplay effect of Pauli-blocking and ph excitations in different dimensions.

DOI: 10.1103/PhysRevA.103.063312

I. INTRODUCTION

A polaron refers to a typical quasiparticle in highly polarized systems. Its concept was first raised by Landau in the 1930s when he discussed how an electron moving through a solid will cause the distortion of the lattice and get trapped [1]. After nearly a century, the concept of a polaron has been well acknowledged and extended to various physical systems. In particular, in recent years ultracold atoms have served as an ideal platform for the study of polaron physics, thanks to the high controllability of species, number, and interaction therein. One important branch of these studies is the Fermi polaron, which describes an impurity immersed in and dressed by a fermionic environment. To date, the attractive and repulsive Fermi polarons have been extensively explored in ultracold atoms both experimentally [2–9] and theoretically [10–36].

For the attractive Fermi polaron in high dimensions, it has been commonly believed that a polaron-to-molecule transition occurs when the attraction between the impurity and majority fermions increases [14–16,18–20,23–26]. Namely, depending on the attraction strength between the impurity and fermions, it could end up with two distinct destinies: one destiny is that the impurity is dressed with the surrounding cloud of majority fermions and forms a fermionic *polaron*; the other is that the impurity essentially binds with one single fermion on top of the Fermi surface to form a bosonic *molecule*. To characterize these distinct pictures, the following variational *Ansatz* for polaron and molecule states with truncated n particle-hole (ph) excitations have been proposed [10,12,13,15–17,20–24,31,34]:

$$P_{2n+1}(0) = \left[\psi_0 c^\dagger_{\mathbf{0}\downarrow} + \sum_{l=1}^{n}\sum_{\mathbf{k}_i\mathbf{q}_j}\psi_{\mathbf{k}_i\mathbf{q}_j} c^\dagger_{\mathbf{P}\downarrow}\prod_{i=1}^{l} c^\dagger_{\mathbf{k}_i\uparrow}\prod_{j=1}^{l} c_{\mathbf{q}_j\uparrow}\right]|\mathrm{FS}\rangle_N, \tag{1}$$

*These authors contributed equally to this work.

†xlcui@iphy.ac.cn

$$M_{2n+2}(0) = \Bigg[\sum_{\mathbf{k}} \phi_{\mathbf{k}} c^{\dagger}_{-\mathbf{k},\downarrow} c^{\dagger}_{\mathbf{k},\uparrow} + \sum_{l=1}^{n} \sum_{\mathbf{k}_i \mathbf{q}_j} \phi_{\mathbf{k}_i \mathbf{q}_j} c^{\dagger}_{\mathbf{P}\downarrow} \times \prod_{i=1}^{l+1} c^{\dagger}_{\mathbf{k}_i\uparrow} \prod_{i=1}^{l} c_{\mathbf{q}_j\uparrow} \Bigg] |\mathrm{FS}\rangle_{N-1}. \quad (2)$$

Here $c^{\dagger}_{\mathbf{k},\sigma}$ is the creation operator of spin-σ fermions at momentum $\mathbf{k}$, the $\downarrow$-spin is the impurity, and $|\mathrm{FS}\rangle_N$ is the Fermi sea of $\uparrow$-spin with number N; all $\mathbf{q}$ ($\mathbf{k}$) are below (above) the Fermi surface of $\uparrow$-atoms and $\mathbf{P} = \sum_j \mathbf{q}_j - \sum_i \mathbf{k}_i$. The two *Ansätzes* above have been shown to lead to a first-order transition between polaron and molecule for both 3D [15,16,18–20] and 2D [23,24] Fermi polaron systems. The same conclusion was also drawn from Monte Carlo methods [14,25,26], where the polaron and molecule were treated separately with their energies extracted from different physical quantities.

The separate treatment of polaron and molecule, though physically inspiring, has its own drawback as the transition appears to be artificially designed at the very beginning. As a result, the conclusion of the polaron-molecule transition can easily get questioned. For instance, a previous theory [36] claimed the absence of such a transition by showing that the two types of variational *Ansätzes* are mutually contained in a generalized momentum space if more ph excitations are included. Therefore, the relation and competition between polaron and molecule deserve a close reexamination under a unified framework.

On the experimental side, the polaron-molecule transition has been identified by a continuous zero-crossing of quasiparticle residue, instead of a sudden jump as in the first-order transition, in both 3D and 2D Fermi gases [2,6]. In particular, a recent experiment on 3D Fermi polarons has observed a smooth evolution of various physical quantities across the polaron-molecule transition, as well as the coexistence of a polaron and molecule near their transition [9]. All these observations need to be reconsidered carefully following the unified treatment of polaron and molecule states.

With the above motivations, in a recent work [37] we have adopted a unified variational method with one ph excitation (V-1ph) to study the Fermi polaron problem in 3D. Specifically, the unified *Ansatz* we used is $P_3(\mathbf{Q})$, i.e., the extension of $P_3(0)$ in Eq. (1) to finite momentum. Note that here momentum $\mathbf{Q}$ is defined in the reference frame of a background Fermi sea of all majority atoms; in other words, it represents the momentum difference between the ground states of an interacting system (Fermi polaron) and a noninteracting system (zero-momentum impurity plus the majority Fermi sea), and thus it can well characterize the interaction effect. By this, we found that the bare molecule state $M_2(0)$ actually constitutes part of $P_3(\mathbf{Q})$ with $|\mathbf{Q}| = k_F$ [denoted as $P_3(k_F)$ for short]; here k_F is the Fermi momentum of majority fermions. Due to the incomplete variational space of $M_2(0)$ even within the lowest-order ph excitations, it always has a higher energy than $P_3(k_F)$. The significance of introducing $M_2(0)$ is found to lie in the strong-coupling regime, where it can serve as a good approximation for $P_3(k_F)$. Within the V-1ph method, we concluded that the nature of the "polaron-molecule transition" is given by an energy competition between $P_3(0)$ and $P_3(k_F)$.

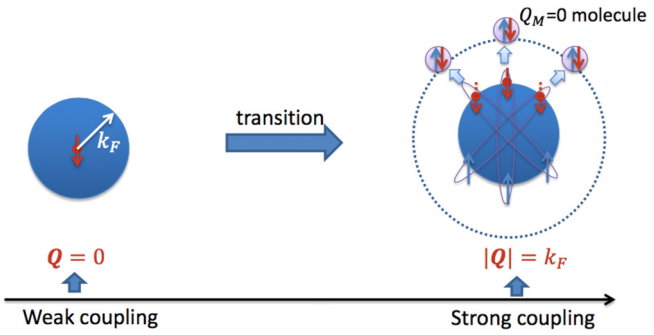

FIG. 1. Illustration of the polaron-molecule transition as changing the impurity ($\downarrow$)-fermion ($\uparrow$) attraction from weak (left side) to strong (right side). In the weak-coupling regime, the ground state is a zero-momentum polaron ($\mathbf{Q} = \mathbf{0}$) dominated by a zero-momentum impurity dressed by particle-hole excitations in the background Fermi sea. In the strong-coupling regime, the ground state switches to $|\mathbf{Q}| = k_F$ in order to facilitate the impurity pairing with a fermion originally at the Fermi surface to form a deeply bound molecule with zero center-of-mass momentum ($Q_M = 0$). This results in a huge ground-state degeneracy in the molecule regime, i.e., SO(3) for 3D and SO(2) for 2D. In this sense, the molecule *Ansatz* $M(0)$ represents a symmetry-breaking state within the degenerate manifold.

This naturally resolves the theoretical debate in Ref. [36] because the transition is between different Q-states rather than between different forms of variational *Ansätzes*. Furthermore, near the transition point, we found the double-minima (at $|\mathbf{Q}| = \mathbf{0}$ and k_F) structure of the impurity dispersion curve, providing the underlying mechanism for polaron-molecule coexistence in realistic systems. Based on this, we qualitatively explained the smooth polaron-molecule transition as observed in the recent experiment [9] with a finite impurity density and at finite temperature.

In the present work, we extend the study of the Fermi polaron problem to various dimensions using the unified variational method with up to two ph excitations (V-2ph), namely under variational *Ansatz* $P_5(\mathbf{Q})$. With the V-2ph method, we confirm the existence of the polaron-molecule transition in 3D and 2D, and we reenforce the conclusion made in Ref. [37] that the nature of such a transition lies in an energy competition between different momenta $\mathbf{Q} = \mathbf{0}$ and $|\mathbf{Q}| = k_F$. Here, we find that the main effect of including two ph excitations is to shift the transition point and the coexistence region to the weaker-coupling regime, from which we obtain a reasonably better prediction to various physical quantities as measured in the weak-coupling and resonance regime of the Fermi polaron experiment [9]. Moreover, we emphasize in this work an important fact that has been overlooked by previous studies, i.e., the molecule ground state has a huge degeneracy [SO(3) for 3D and SO(2) for 2D]. The recognition of such degeneracy is crucially important for correctly evaluating the individual occupation of polaron and molecule in their coexistence region for realistic Fermi polaron systems. In Fig. 1, we illustrate the nature of the polaron-molecule transition as well as the origin of the huge ground-state degeneracy for molecules.

To further check the validity of our results in 2D, we adopt a different variational method based on the Gaussian sample

of high-order ph excitations (V-Gph) [38], which gives the same conclusion for the nature of polaron-molecule transition therein. For a 1D system, the V-2ph method predicts no sharp transition and the ground state is always the $Q = 0$ state for any coupling strength, consistent with the Bethe-*Ansatz* solutions. These comparisons further justify the validity of the V-2ph method and the reliability of our results in various dimensions. We analyze that the presence or absence of the polaron-molecule transition is closely related to the interplay effect of Pauli-blocking and ph excitations in different dimensions.

The rest of the paper is organized as follows. In Sec. II, we present the algorithm from two variational *Ansätzes* to treat the Fermi polaron problem: one is the variational *Ansatz* with up to two ph excitations (V-2ph), and the other is the Gaussian variational *Ansatz* with high-order ph excitations (V-Gph). In Sec. III, we present the results of the polaron-molecule transition for single-impurity system in various dimensions from the two methods, and we analyze the intrinsic reason for the presence/absence of such a transition in different dimensions. In Sec. IV, we use the single-impurity results to investigate the coexistence and smooth crossover between polaron and molecule in 3D Fermi polaron systems, in comparison with the experimental data from Ref. [9]. Finally the results are summarized in Sec. V.

II. METHODS

We consider the following Hamiltonian describing a spin-$\downarrow$ impurity interacting with spin-$\uparrow$ majority fermions:

$$H = \sum_{\mathbf{k}\sigma} \epsilon_{\mathbf{k},\sigma} c^\dagger_{\mathbf{k}\sigma} c_{\mathbf{k}\sigma} + g/L^d \sum_{\mathbf{Q},\mathbf{k},\mathbf{k}'} c^\dagger_{\mathbf{Q}-\mathbf{k},\uparrow} c^\dagger_{\mathbf{k},\downarrow} c_{\mathbf{k}',\downarrow} c_{\mathbf{Q}-\mathbf{k}',\uparrow} \quad (3)$$

where $\epsilon_{\mathbf{k}} = \mathbf{k}^2/(2m)$, d is the dimension of the system, and g is the bare coupling constant, which needs to be renormalized in 2D and 3D due to the induced ultraviolet divergence in two-body scattering process. Specifically, for 3D, g is related to the s-wave scattering length a_s via $1/g = m/(4\pi a_s) - 1/V \sum_{\mathbf{k}} 1/(2\epsilon_{\mathbf{k}})$ with $V = L^3$ the volume of the system; for 2D, the scattering length a_{2d} defines the two-body binding energy $E_{2b} = -1/ma^2_{2d}$, and g is related to E_{2b} via $1/g = -1/S \sum_{\mathbf{k}} 1/(2\epsilon_{\mathbf{k}} - E_{2b})$, where $S = L^2$ is the area of the system. In this work, we take $\hbar$ as unity for brevity.

In this section, we present the algorithm of two variational methods used to treat Fermi polaron problems. One is the unified variational *Ansatz* $P_5(\mathbf{Q})$ with up to two ph excitations (V-2ph), in comparison with the molecule *Ansatz* $M_4(\mathbf{Q}_M)$. The other is the Gaussian variational *Ansatz* with high-order ph excitations (V-Gph).

A. Unified variational approach with up to two ph excitations (V-2ph)

In the following, we will present the algorithm of $P_5(\mathbf{Q})$, the polaron *Ansatz* with arbitrary momentum and with up to two ph excitations, as well as the algorithm of $M_4(\mathbf{Q}_M)$, the molecule *Ansatz* with arbitrary momentum and with one ph excitation. It is noted that the $\mathbf{Q} = \mathbf{0}$ case of $P_5(\mathbf{Q})$ has been studied previously in 3D [13,15], 2D [24], and 1D [29] Fermi polaron systems; the $\mathbf{Q}_M = \mathbf{0}$ case of $M_4(\mathbf{Q}_M)$ has also been studied previously in 3D [15–17] and 2D [23,24] systems. Here we generalize the study to arbitrarily finite momenta, which involves more numerical work than the zero-momentum case. The intrinsic relation between the two *Ansätzes* will also be discussed.

1. $P_5(\mathbf{Q})$

The generalized polaron *Ansatz* with up to two ph excitations is

$$P_5(\mathbf{Q}) = \Bigg[\psi_0 c^\dagger_{\mathbf{Q}\downarrow} + \sum_{\mathbf{kq}} \psi_{\mathbf{kq}} c^\dagger_{\mathbf{Q}+\mathbf{q}-\mathbf{k}\downarrow} c^\dagger_{\mathbf{k}\uparrow} c_{\mathbf{q}\uparrow} + \frac{1}{4} \sum_{\mathbf{kk'qq'}} \psi_{\mathbf{kk'qq'}} c^\dagger_{\mathbf{Q}+\mathbf{q}+\mathbf{q}'-\mathbf{k}-\mathbf{k}'\downarrow} c^\dagger_{\mathbf{k}\uparrow} c^\dagger_{\mathbf{k}'\uparrow} c_{\mathbf{q}\uparrow} c_{\mathbf{q}'\uparrow} \Bigg] |\mathrm{FS}\rangle_N. \quad (4)$$

By imposing the Schrödinger equation, we can obtain the coupled integral equations for all variational coefficients, from which the ground-state energy can be obtained. This is equivalent to minimizing the energy functional $E_{\mathrm{tot}} = \langle H \rangle$ for a normalized *Ansatz*. In this paper, we take the unperturbed Fermi sea $|\mathrm{FS}\rangle_N$ as the reference system and define the impurity energy as $E = E_{\mathrm{tot}} - E_{\mathrm{FS}}$, with E_{FS} the energy of $|\mathrm{FS}\rangle_N$.

The equations for the variational coefficients are

$$-\frac{1}{g}\left(E - E^{(0)}_{\mathbf{Q}}\right)\psi_0 = \sum_{\mathbf{kq}} \psi_{\mathbf{kq}}, \quad (5)$$

$$-\frac{1}{g}\left(E - E^{(1)}_{\mathbf{kq}}\right)\psi_{\mathbf{kq}} = \psi_0 + \sum_{\mathbf{K}} \psi_{\mathbf{Kq}} - \sum_{\mathbf{q}'} \psi_{\mathbf{kq}'} - \sum_{\mathbf{Kq}'} \psi_{\mathbf{kKqq}'}, \quad (6)$$

$$-\frac{1}{g}\left(E - E^{(2)}_{\mathbf{kk'qq'}}\right)\psi_{\mathbf{kk'qq'}} = -\psi_{\mathbf{kq}} - \psi_{\mathbf{k'q'}} + \psi_{\mathbf{kq}'} + \psi_{\mathbf{k'q}} + \sum_{K} \psi_{\mathbf{Kk'qq'}} + \sum_{\mathbf{K}} \psi_{\mathbf{kKqq'}} - \sum_{\mathbf{Q}'} \psi_{\mathbf{kk'Q'q'}} - \sum_{\mathbf{Q}'} \psi_{\mathbf{kk'qQ'}}, \quad (7)$$

where $E^{(0)}_{\mathbf{Q}} = \epsilon_{\mathbf{Q}}$, $E^{(1)}_{\mathbf{kq}} = \epsilon_{\mathbf{Q}+\mathbf{q}-\mathbf{k}} + \epsilon_{\mathbf{k}} - \epsilon_{\mathbf{q}}$, $E^{(2)}_{\mathbf{kk'qq'}} = \epsilon_{\mathbf{Q}+\mathbf{q}+\mathbf{q}'-\mathbf{k}-\mathbf{k}'} + \epsilon_{\mathbf{k}} + \epsilon_{\mathbf{k}'} - \epsilon_{\mathbf{q}} - \epsilon_{\mathbf{q}'}$. As before, all $\mathbf{q}$ ($\mathbf{k}$) in these equations are by default below (above) the Fermi surface of $|\mathrm{FS}\rangle_N$.

The above equations can be solved in 1D using the iterative method. For 2D and 3D, due to the renormalization scheme of bare coupling g, the equations can be simplified by using

$$g\sum_{k'}\frac{\alpha_{\mathbf{k}'\mathbf{q}}}{E-E^{(2)}_{\mathbf{k}\mathbf{k}'\mathbf{q}\mathbf{q}'}}\sim 0,$$
$$g\sum_{k'}\frac{1}{E-E^{(2)}_{\mathbf{k}\mathbf{k}'\mathbf{q}\mathbf{q}'}}\sim 1.$$

The final equations for numerical simulation are

$$E=\epsilon_{\mathbf{Q}}+\sum_{\mathbf{q}}A_{\mathbf{q}}, \tag{8}$$
$$\alpha_{\mathbf{k}\mathbf{q}}=\frac{A_{\mathbf{q}}-\sum_{\mathbf{q}'}G(\mathbf{k},\mathbf{q},\mathbf{q}')}{E-E^{(1)}_{\mathbf{k}\mathbf{q}}}, \tag{9}$$
$$G(\mathbf{k},\mathbf{q},\mathbf{q}')=\frac{\alpha_{\mathbf{k}\mathbf{q}'}-\alpha_{\mathbf{k}\mathbf{q}}-\sum_{\mathbf{k}'}\frac{G(\mathbf{k}',\mathbf{q},\mathbf{q}')}{E-E^{(2)}_{\mathbf{k}\mathbf{k}'\mathbf{q}\mathbf{q}'}}}{h(\mathbf{k},\mathbf{q},\mathbf{q}')}, \tag{10}$$

with

$$A_{\mathbf{q}}=\frac{1-\sum_{\mathbf{k}\mathbf{q}'}\frac{G(\mathbf{k},\mathbf{q},\mathbf{q}')}{E-E^{(1)}_{\mathbf{k}\mathbf{q}}}}{h(\mathbf{q})}, \tag{11}$$
$$h(\mathbf{q})=\frac{1}{g}-\sum_{\mathbf{k}}\frac{1}{E-E^{(1)}_{\mathbf{k}\mathbf{q}}}, \tag{12}$$
$$h(\mathbf{k},\mathbf{q},\mathbf{q}')=\frac{1}{g}-\sum_{\mathbf{k}'}\frac{1}{E-E^{(2)}_{\mathbf{k}\mathbf{k}'\mathbf{q}\mathbf{q}'}}, \tag{13}$$

where we have defined $\alpha_{\mathbf{k}\mathbf{q}}=\psi_{\mathbf{k}\mathbf{q}}/\psi_0$, $A_{\mathbf{q}}=g(1+\sum_{\mathbf{k}}\alpha_{\mathbf{k}\mathbf{q}})$, and $G(\mathbf{k},\mathbf{q},\mathbf{q}')=g\sum_{\mathbf{k}'}\psi_{\mathbf{k}\mathbf{k}'\mathbf{q}\mathbf{q}'}/\psi_0$.

Due to the rotational invariance of momentum $\mathbf{Q}$, in this work we have taken it along the z axis for simplicity. Compared to the zero-momentum case, here the finite $\mathbf{Q}$ in 3D and 2D introduces more momentum variables in the simulation and thus requires a larger amount of numerical work. In practice, we have used an iterative scheme to solve Eqs. (8)–(10). In updating E in Eq. (8) and updating $G(\mathbf{k},\mathbf{q},\mathbf{q}')$ in Eq. (10), we have used the successive overrelaxation method to reduce the fluctuation and ensure the convergency of the results.

2. $M_4(\mathbf{Q}_M)$

The generalized molecule *Ansatz* with one ph excitation is written as

$$M_4(\mathbf{Q}_{\mathrm{M}})=\left[\sum_{\mathbf{k}}\phi_{\mathbf{k}}c^{\dagger}_{\mathbf{Q}_{\mathrm{M}}-\mathbf{k},\downarrow}c^{\dagger}_{\mathbf{k},\uparrow}+\frac{1}{2}\sum_{\mathbf{k}\mathbf{k}'\mathbf{q}}\phi_{\mathbf{k}\mathbf{k}'\mathbf{q}}c^{\dagger}_{\mathbf{Q}_{\mathrm{M}}+\mathbf{q}-\mathbf{k}-\mathbf{k}'\downarrow}c^{\dagger}_{\mathbf{k}\uparrow}c^{\dagger}_{\mathbf{k}'\uparrow}c_{\mathbf{q}\uparrow}\right]|\mathrm{FS}\rangle_{N-1}. \tag{14}$$

By imposing the Schrödinger equation, one can obtain the equations for all variables $\phi_{\mathbf{k}}$, $\phi_{\mathbf{k}\mathbf{k}'\mathbf{q}}$. Again for the 2D and 3D cases, the equations can be simplified. Namely, by introducing two auxiliary functions $\gamma=g\sum_{\mathbf{k}}\phi_{\mathbf{k}}$ and $\eta_{\mathbf{k}\mathbf{q}}=g\sum_{\mathbf{k}'}\phi_{\mathbf{k}\mathbf{k}'\mathbf{q}}$, we can arrive at the following integral equations for $\tilde{\eta}_{\mathbf{k}\mathbf{q}}=\eta_{\mathbf{k}\mathbf{q}}/\gamma$ (see the $Q_{\mathrm{M}}=0$ case in [15,16,23,24]):

$$\frac{1}{g}-\sum_{\mathbf{k}}\frac{1}{E+E_F-E^{(1)}_{\mathbf{k}}}=\sum_{\mathbf{k}\mathbf{q}}\frac{\tilde{\eta}_{\mathbf{k}\mathbf{q}}}{E+E_F-E^{(1)}_{\mathbf{k}}}, \tag{15}$$

$$\left[\frac{1}{g}-\sum_{\mathbf{k}'}\frac{1}{E+E_F-E^{(2)}_{\mathbf{k}\mathbf{k}'\mathbf{q}}}\right]\tilde{\eta}_{\mathbf{k}\mathbf{q}}=-\frac{1+\sum_{\mathbf{q}'}\tilde{\eta}_{\mathbf{k}\mathbf{q}'}}{E-E^{(1)}_{\mathbf{k}}}-\sum_{\mathbf{k}'}\frac{\tilde{\eta}_{\mathbf{k}\mathbf{q}}}{E+E_F-E^{(2)}_{\mathbf{k}\mathbf{k}',\mathbf{q}}}, \tag{16}$$

with $E^{(1)}_{\mathbf{k}}=\epsilon_{\mathbf{Q}_M-\mathbf{k}}+\epsilon_{\mathbf{k}}$ and $E^{(2)}_{\mathbf{k}\mathbf{k}',\mathbf{q}}=\epsilon_{\mathbf{Q}_M-\mathbf{k}-\mathbf{k}'+\mathbf{q}}+\epsilon_{\mathbf{k}}+\epsilon_{\mathbf{k}'}-\epsilon_{\mathbf{q}}$.

Again in the calculation we take $\mathbf{Q}_M$ along the z axis due to its rotational invariance. Compared to $P_5(\mathbf{Q})$, the simulation of $M_4(\mathbf{Q}_M)$ is easier due to the smaller variational space. One can obtain the molecule energy E either by using the iterative method or by solving large matrix equations with respect to $\tilde{\eta}_{\mathbf{k}\mathbf{q}}$. We have confirmed that these two methods produce consistent results.

3. Relation between $P_5(\mathbf{Q})$ and $M_4(\mathbf{Q}_M)$

In our previous work [37], we have discussed the intimate relation between $M_2(0)$ and $P_3(\mathbf{Q})$ with $|\mathbf{Q}|=k_F$. The discussion can be straightforwardly extended to other momentum sectors and to arbitrary levels of ph excitations. Here we consider the case of $P_5(\mathbf{Q})$ and $M_4(\mathbf{Q}_M)$ and discuss their relation as below. We start with the following equality between two Fermi sea states:

$$|\mathrm{FS}\rangle_{N-1}=c_{\mathbf{k}_F\uparrow}|\mathrm{FS}\rangle_N. \tag{17}$$

Here $\mathbf{k}_F$ is the Fermi momentum that can point to any direction on the Fermi surface. Given (17), one can see that if we further take

$$\psi_0=0,\quad \psi_{\mathbf{k}\mathbf{q}}=\phi_{\mathbf{k}}\delta_{\mathbf{q},\mathbf{k}_F},\quad \psi_{\mathbf{k}\mathbf{k}'\mathbf{q}\mathbf{q}'}=\phi_{\mathbf{k}\mathbf{k}'\mathbf{q}}\delta_{\mathbf{q}',\mathbf{k}_F}, \tag{18}$$

then $P_5(\mathbf{Q})$ in (4) exactly reproduces $M_4(\mathbf{Q}_{\mathrm{M}})$ in (14) under the relation

$$\mathbf{Q}_{\mathrm{M}}=\mathbf{Q}+\mathbf{k}_F. \tag{19}$$

Equations (18) and (19), which can be directly generalized to arbitrary order of ph excitations, immediately tell us two important facts:

(i) $M_4(\mathbf{Q}_{\mathrm{M}})$ has a smaller variational space than $P_5(\mathbf{Q}=\mathbf{Q}_{\mathrm{M}}-\mathbf{k}_F)$. Specifically, the former corresponds to only considering a particular configuration of ph excitations in the latter, i.e., with one hole pinning at the Fermi surface [see Eq. (18)]. In principle, such a configuration is not isolated and can be coupled to other ph excitations via interactions, which will further reduce the variational energy. Due to such incomplete variational space, $M_4(\mathbf{Q}_{\mathrm{M}})$ always has a higher variational energy than $P_5(\mathbf{Q}=\mathbf{Q}_{\mathrm{M}}-\mathbf{k}_F)$ for the ground state of the system. When reduced to the special case $\mathbf{Q}_{\mathrm{M}}=\mathbf{0}$ and $|\mathbf{Q}|=k_F$, we arrive at the conclusion that $M_4(0)$ always produces a higher energy than $P_5(\mathbf{Q})$ with $|\mathbf{Q}|=k_F$. This is a direct extension of the conclusion in our previous work with one ph excitation [37].

(ii) The correspondence (19) tells that the previously studied *zero-momentum* molecule $M(0)$ actually stays in a different momentum sector from the *zero-momentum* polaron $P(0)$. Such a momentum difference, $\mathbf{k}_F$, which originates from the relation (17) between two Fermi seas $|\mathrm{FS}\rangle_N$ and $|\mathrm{FS}\rangle_{N-1}$, is robust against the choice of reference state. Nevertheless, to correctly characterize the status of the impurity, it is important to choose the reference state as $|\mathrm{FS}\rangle_N$, instead of $|\mathrm{FS}\rangle_{N-1}$. By choosing $|\mathrm{FS}\rangle_N$ as the reference state, the momenta of $P(0)$ and $M(0)$ are, respectively, $\mathbf{Q}=\mathbf{0}$ and $\mathbf{Q}=-\mathbf{k}_F$, giving the momentum difference $\mathbf{k}_F$. Because of such a momentum difference, $M(0)$ and $P(0)$ should have zero overlap [note that the Hamiltonian (3) preserves the total momentum]. Recognizing such a difference is crucially important for understanding the nature of the polaron-molecule transition, as addressed in Sec. III.

Based on (i) and (ii), we can conclude that up to two ph excitations, the generalized polaron *Ansatz* $P_5(\mathbf{Q})$ can serve as the unified variational wave function for both polaron and molecule states. The ground state of the system can then be obtained by searching for the energy minimum in the $\mathbf{Q}$-space.

B. Gaussian variational method with high-order particle-hole excitations (V-Gph)

For a 2D system, besides the V-2ph method we adopt the Gaussian variational method with high-order ph excitations (V-Gph) [38]. The essence of this method is the combination of a fermionic Gaussian state [39,40] and the Lee-Low-Pines (LLP) transformation [41]. To be self-contained, in the following we give a brief introduction to this method.

Applying the LLP transformation $U_{\mathrm{LLP}}=e^{-i\hat{\mathbf{K}}\hat{\mathbf{r}}}$, where $\hat{\mathbf{K}}=\sum_{\mathbf{k}}\mathbf{k}c^{\dagger}_{\mathbf{k}\uparrow}c_{\mathbf{k}\uparrow}$ is the total momentum of the background spin-up atoms and $\hat{\mathbf{r}}$ is the coordinate of the impurity, the Hamiltonian (3) can be transformed as

$$\begin{aligned}H_{\mathrm{LLP}}&=U^{\dagger}_{\mathrm{LLP}}HU_{\mathrm{LLP}}\\&=\sum_{\mathbf{k}}(\epsilon_{\mathbf{k}}-\mu)c^{\dagger}_{\mathbf{k}\uparrow}c_{\mathbf{k}\uparrow}+\frac{\hat{\mathbf{p}}^2}{2m}-\sum_{\mathbf{k}}\frac{\hat{\mathbf{p}}\cdot\mathbf{k}}{m}c^{\dagger}_{\mathbf{k}\uparrow}c_{\mathbf{k}\uparrow}\\&\quad+\sum_{\mathbf{k},\mathbf{k}'}\frac{\mathbf{k}\cdot\mathbf{k}'}{2m}c^{\dagger}_{\mathbf{k}\uparrow}c_{\mathbf{k}\uparrow}c^{\dagger}_{\mathbf{k}'\uparrow}c_{\mathbf{k}'\uparrow}+\frac{g}{L^2}\sum_{\mathbf{k},\mathbf{k}'}c^{\dagger}_{\mathbf{k}\uparrow}c_{\mathbf{k}'\uparrow}.\end{aligned}\tag{20}$$

Here $\hat{\mathbf{p}}$ is the momentum operator of the impurity. Note that here we have introduced an additional term "$-\mu\sum_{\mathbf{k}}c^{\dagger}_{\mathbf{k}\uparrow}c_{\mathbf{k}\uparrow}$" into the original Hamiltonian Eq. (3) to tune the particle number of the background Fermi sea. After the LLP transformation, the conserved total momentum of the system transforms into the momentum of the impurity, i.e.,

$$U^{\dagger}_{\mathrm{LLP}}(\hat{\mathbf{p}}+\hat{\mathbf{K}})U_{\mathrm{LLP}}=\hat{\mathbf{p}}.\tag{21}$$

Thus we can replace $\hat{\mathbf{p}}$ in H_{LLP} with its eigenvalue $\mathbf{Q}$, which eliminates the degree of the impurity.

We further use fermionic Gaussian state to approximate the ground state with total momentum $\mathbf{Q}$ of the transformed Hamiltonian, Eq. (20). The fermionic Gaussian state is defined as

$$|\Psi_{\mathrm{GS}}\rangle=c^{\dagger}_{\mathbf{Q}\downarrow}U_{\mathrm{GS}}|0\rangle,\tag{22}$$

where $|0\rangle$ is chosen to be the vacuum state and

$$U_{\mathrm{GS}}=e^{i\frac{1}{4}A^T\xi A}\tag{23}$$

is called the Gaussian unitary operator, $A=(a_{1,\mathbf{k}_1},\ldots,a_{1,\mathbf{k}_{N_k}},a_{2,\mathbf{k}_1},\ldots,a_{2,\mathbf{k}_{N_k}})^T$, N_k is the number of $\mathbf{k}$ modes satisfying $|\mathbf{k}|\leqslant k_c$ with cutoff k_c, the Majorana operators are defined as $a_{1,\mathbf{k}_j}=c^{\dagger}_{\mathbf{k}_j,\uparrow}+c_{\mathbf{k}_j,\uparrow}$, $a_{2,\mathbf{k}_j}=i(c^{\dagger}_{\mathbf{k}_j,\uparrow}-c_{\mathbf{k}_j,\uparrow})$, and the variational parameter ξ is an antisymmetric Hermitian matrix which has $2N_k^2-2N_k$ free matrix elements. We point out that the use of Majorana operators is just for computational convenience, and the operators can be re-expressed in terms of $c^{\dagger}_{\mathbf{k}_j,\uparrow}$ and $c_{\mathbf{k}_j,\uparrow}$ as in Ref. [42].

To eliminate the gauge degree of freedom in ξ, it is convenient to introduce a covariance matrix [38]

$$(\Gamma)_{s_1,\mathbf{k}_1;s_2,\mathbf{k}_2}=\frac{i}{2}\langle\Psi_{\mathrm{GS}}|[a_{s_1,\mathbf{k}_1},a_{s_2,\mathbf{k}_2}]|\Psi_{\mathrm{GS}}\rangle,\tag{24}$$

with $s_1(s_2)=1,2$. The covariance matrix is related to ξ as

$$\Gamma=-U_m\begin{pmatrix}\mathbf{0}&-\mathbf{1}_{N_k}\\\mathbf{1}_{N_k}&\mathbf{0}\end{pmatrix}U_m^T,\tag{25}$$

where $U_m=e^{i\xi}$ and $\mathbf{1}_{N_k}$ is the identity matrix of dimension N_k.

By reversing the LLP transformation, the eigenstate of the original Hamiltonian (3) with a total conserved momentum $\mathbf{Q}$ can be expressed as a non-Gaussian state

$$|\Psi\rangle=U_{\mathrm{LLP}}c^{\dagger}_{\mathbf{Q}\downarrow}U_{\mathrm{GS}}|0\rangle.\tag{26}$$

The imaginary-time evolution equation for the non-Gaussian state Eq. (26) can be written as

$$d_\tau|\Psi\rangle=-\mathcal{P}(H-E_{\mathrm{tot}})|\Psi\rangle,\tag{27}$$

where $\mathcal{P}$ is the projection operator onto the subspace spanned by tangent vectors of the variational manifold, and $E_{\mathrm{tot}}=\langle\Psi|H|\Psi\rangle$ can be calculated using Wick's theorem. Finally, we obtain

$$\begin{aligned}E_{\mathrm{tot}}&=\frac{1}{2}\sum_{\mathbf{k}}\varepsilon_{\mathbf{k}}-\frac{\mu N_{\mathbf{k}}}{2}+\frac{1}{4}\sum_{\mathbf{k}}\left(\varepsilon_{\mathbf{k}}-\mu-\frac{\mathbf{Q}\cdot\mathbf{k}}{m}\right)(\Gamma_{1,\mathbf{k};2,\mathbf{k}}-\Gamma_{2,\mathbf{k};1,\mathbf{k}})+\frac{\mathbf{Q}^2}{2m}\\&\quad+\frac{g}{2L^2}N_{\mathbf{k}}+\frac{g}{4L^2}\sum_{\mathbf{k},\mathbf{k}'}(\Gamma_{1,\mathbf{k};2,\mathbf{k}'}-\Gamma_{2,\mathbf{k};1,\mathbf{k}'})+\frac{1}{8m}\sum_{\mathbf{k}}\mathbf{k}^2\\&\quad+\frac{1}{32m}\left[\sum_{\mathbf{k}}\mathbf{k}(\Gamma_{1,\mathbf{k};2,\mathbf{k}}-\Gamma_{2,\mathbf{k};1,\mathbf{k}})\right]^2-\frac{1}{8m}\sum_{\mathbf{k},\mathbf{k}'}\mathbf{k}\cdot\mathbf{k}'\Gamma_{1,\mathbf{k};1,\mathbf{k}'}\Gamma_{2,\mathbf{k};2,\mathbf{k}'}+\frac{1}{8m}\sum_{\mathbf{k},\mathbf{k}'}\mathbf{k}\cdot\mathbf{k}'\Gamma_{1,\mathbf{k};2,\mathbf{k}'}\Gamma_{2,\mathbf{k};1,\mathbf{k}'}.\end{aligned}\tag{28}$$

To be consistent with the variational approach with truncated ph excitations, we calculate the energy $E = E_{\rm tot} + \mu N_\uparrow - E_{\rm FS}$. The imaginary-time equation of motion (EOM) for the covariance matrix Γ is

$$\partial_\tau \Gamma = -h - \Gamma h \Gamma, \tag{29}$$

with

$$h = 4\frac{\delta E_{\rm GS}}{\delta \Gamma}. \tag{30}$$

Evolving Γ according to Eq. (29) until the variational energy converges, we can finally obtain the approximated ground state.

Now we discuss the level of ph excitations in V-Gph. Since the Fermi sea $|{\rm FS}\rangle_N$ is also a Gaussian state, we can replace $|0\rangle$ as $|{\rm FS}\rangle_N$ in Eq. (22) and immediately one can see that it can include multiple ph excitations. By expanding $U_{\rm GS}$ in terms of ξ: $U_{\rm GS} = 1 + i\frac{1}{4}A^T\xi A + \cdots$, the wave function Ψ can also be expanded in terms of ξ. We note that the first two terms in the expansion have included all the bare and one ph excitation terms in $P_3(\mathbf{Q})$, while the coefficients of two and higher ph excitation terms in Ψ are strongly correlated with those of one ph terms and thus are not free variables. This means that V-Gph can be a better variational approach than V-1ph, but not necessarily better than V-2ph. In this work, we use it as a complementary method to test the reliability of V-2ph.

III. POLARON-MOLECULE TRANSITION/CROSSOVER FOR SINGLE-IMPURITY SYSTEMS

In this section, we study the polaron-to-molecule transition or crossover for single-impurity systems in various dimensions. We will apply the V-2ph method for all dimensions, in combination with the V-Gph method for 2D and the Bethe-*Ansatz* method for 1D. The conclusions for the presence/absence of the polaron-molecule transition from these methods are consistent.

A. 3D

In our previous work [37], we have used the V-1ph method based on *Ansatz* $P_3(\mathbf{Q})$ to unveil the nature of the polaron-molecule transition in 3D. Here by using the V-2ph method with up to two ph excitations, we will reexamine the polaron and molecule physics in this system. In our numerical simulations, we have taken the momentum cutoff as $k_c = 30k_F$.

First, we investigate the relation between $M_4(0)$ and $P_5(\mathbf{Q})$ with $\mathbf{Q} = k_F\mathbf{e}_z$, and we will denote the latter state as $P_5(k_F)$ for short. As discussed in the preceding section, due to the incomplete variational space of $M_4(0)$, it should be energetically unfavorable as compared to $P_5(k_F)$. In Fig. 2, we show their energies, in comparison with $P_3(k_F)$ and $M_2(0)$, as functions of coupling strength. It is found that the molecule state $M_4(0)$ [or $M_2(0)$] always has a higher energy than $P_5(k_F)$ [or $P_3(k_F)$], as expected. Only in the strong-coupling side does the energy difference between $M_4(0)$ and $P_5(k_F)$ [or between $M_2(0)$ and $P_3(k_F)$] become invisible. For instance, $M_4(0)$ energetically approaches $P_5(k_F)$ at couplings $1/(k_F a_s) \gtrsim 0.3$, and $M_2(0)$ energetically approaches $P_3(k_F)$ at $1/(k_F a_s) \gtrsim 0.6$. Moreover, we can see that the V-2ph method produces a lower energy for both polaron and molecule states, as compared to those from the V-1ph method.

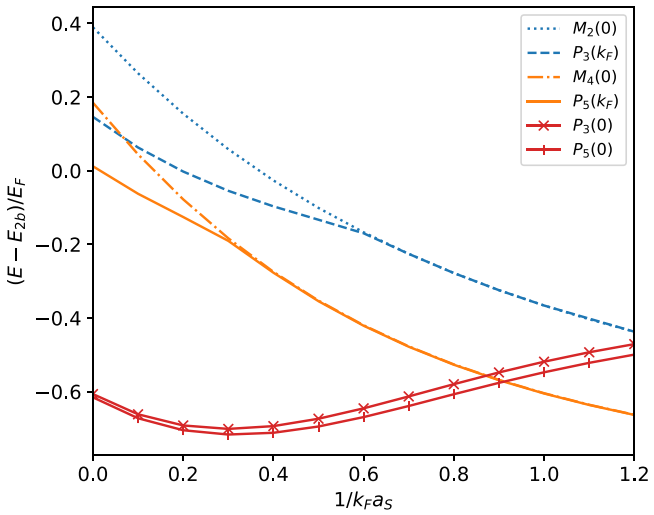

FIG. 2. Energy comparison between various *Ansätzes* for a 3D single-impurity system. All energies are shifted by $E_{2b} = -1/(ma_s^2)$ in $a_s > 0$ in order to highlight the difference.

To explain why the energies of $M_4(0)$ and $P_5(k_F)$ become so close in the strong-coupling limit, we examine the wave function of $P_5(k_F)$ in Fig. 3. Specifically, we show the hole angular distribution of variational coefficients at two different coupling strengths. It is found that at intermediate coupling, $1/k_F a_s = 0.2$, the angular distribution of the hole ($\mathbf{q}$) spreads in a broad region, while at stronger coupling, $1/k_F a_s = 0.9$, the distribution shows a pronounced peak at $\theta_q = \pi$, i.e., along the opposite direction of $\mathbf{Q}$ ($= k_F\mathbf{e}_z$). Recalling Eqs. (18) and (19), this corresponds to locking the

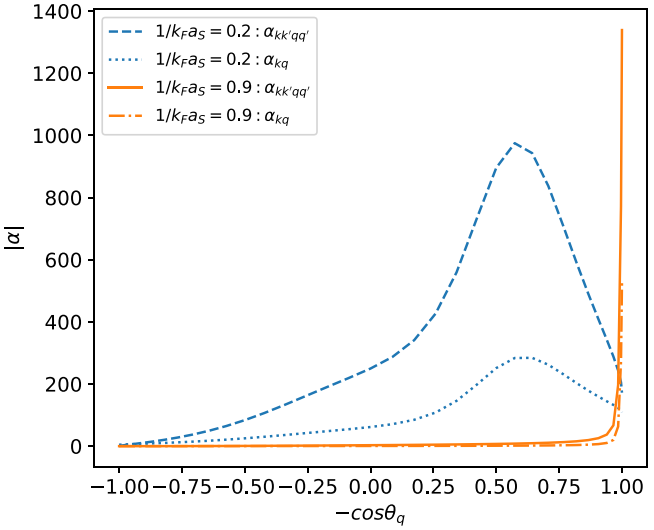

FIG. 3. Hole angular distribution of variational coefficients in $P_5(k_F)$ at different coupling strengths. Here we use the polar coordinate $(|\mathbf{k}|, \theta_k, \phi_k)$ to characterize momentum $\mathbf{k}$, with $\theta_k \in [0, \pi)$ and $\phi_k \in [0, 2\pi)$. In the figure we choose $\mathbf{k} = (1.32k_F, 0.53, 0.44)$, $\mathbf{k}' = (2.64k_F, 0.53, 0.44)$, $\mathbf{q}' = (k_F, 0, 0.44)$, and $\mathbf{q} = (k_F, \theta_q, 0.44)$ in $\alpha_{\mathbf{kq}} \equiv \psi_{\mathbf{kq}}/\psi_0$ and $\alpha_{\mathbf{kk'qq'}} \equiv \psi_{\mathbf{kk'qq'}}/\psi_0$.

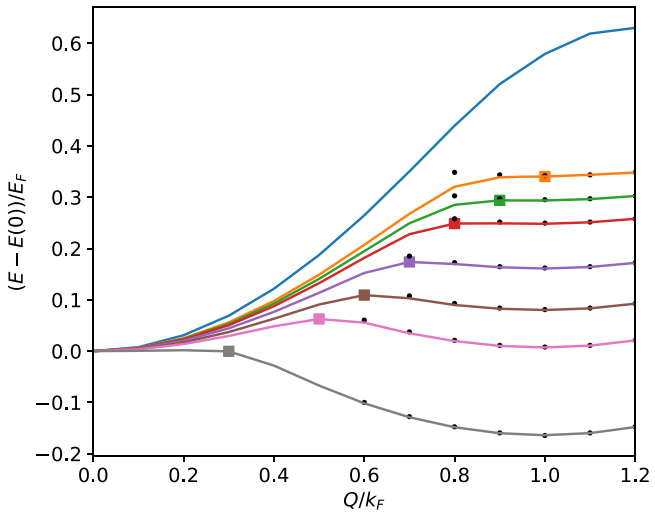

FIG. 4. (a) Energy dispersion of $P_5(\mathbf{Q})$ (solid lines) in 3D at various couplings (from top to bottom) $1/(k_F a_s) = 0.2, 0.5, 0.55, 0.6, 0.7, 0.8, 0.9, 1.2$, shifted by the value at $\mathbf{Q} = \mathbf{0}$. The rectangular point marks the position of maximum energy, and the small black dots show the energies of $M_4(\mathbf{Q}_M)$, with $|\mathbf{Q}_M|$ shifted by k_F in order to compare with the energies of $P_5(\mathbf{Q})$. Here $Q = |\mathbf{Q}|$.

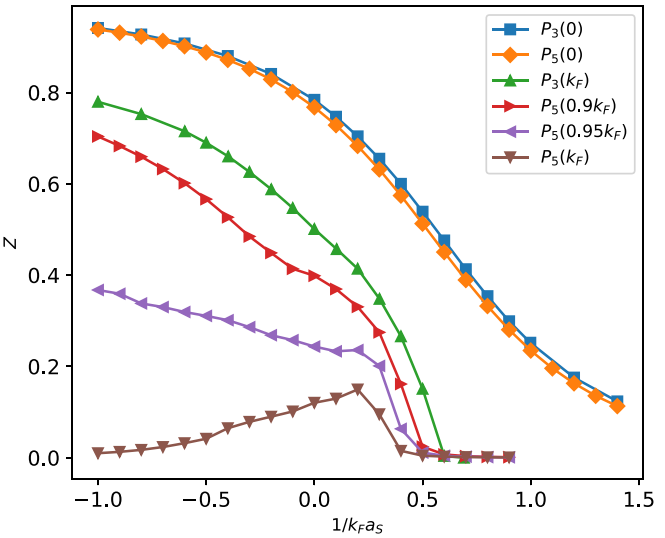

FIG. 5. Residue Z as a function of coupling strength $1/(k_F a_s)$ for different momentum states using V-1ph or V-2ph methods.

hole at $-\mathbf{Q}$ so as to produce a molecule state with $\mathbf{Q}_M = \mathbf{0}$. We have checked that such a pronounced hole distribution at $-\mathbf{Q}$ applies for general excited momenta $\mathbf{k}$ and $\mathbf{k}'$. Together with the energy resemblance as shown in Fig. 2, this serves as strong evidence that $M_4(0)$ indeed can well approximate $P_5(k_F)$ in the strong-coupling limit.

Given the fact that the molecule $M_4(0)$ is merely a good approximation for the finite-momentum state $P_5(k_F)$, we are now ready to investigate the polaron-molecule competition by examining the energy dispersion $E(Q)$ from $P_5(\mathbf{Q})$, with $Q = |\mathbf{Q}|$ (in our numerical calculation, we have taken $\mathbf{Q}$ along the z-direction). In Fig. 4, we show $E(Q)$ for various coupling strengths. We can see that for weak coupling, $1/(k_F a_s) \lesssim 0.5$, there is only one minimum in the dispersion, and the $Q = 0$ polaron is the only ground state. Near $\mathbf{Q} \sim \mathbf{0}$, one has

$$E(Q) = \epsilon_P + \frac{\mathbf{Q}^2}{2m_P^*}, \tag{31}$$

with $\epsilon_P = E(0)$ and m_P^* denoting the energy and effective mass of the polaron state, respectively. As $1/(k_F a_s)$ increases to ~0.5 and beyond, another minimum appears at $Q = k_F$ as a metastable state. At $1/k_F a_s = 0.91$, the two minima have the same energy, signifying a first-order transition between $Q = 0$ and $Q = k_F$ states, or between polaron and molecule states given that $M_4(0)$ can well approximate $P_5(k_F)$ near the transition (see black dots). At even stronger attractions, the local minimum at $Q = 0$ is bent downward, and the only stable state is at $Q = k_F$, the molecule state. It is found that near the local minimum $Q \sim k_F$, the dispersion follows

$$E(Q) = \epsilon_M + \frac{(|\mathbf{Q}| - k_F)^2}{2m_M^*}, \tag{32}$$

with $\epsilon_M = E(k_F)$ and m_M^*, respectively, the energy and effective mass of the molecule state. Here with the V-2ph method, the double minima structure of the dispersion appears in the coupling window $1/k_F a_s \in (0.5, 1.2)$, moving to the weaker-coupling side as compared to the double minima region from the V-1ph method [37].

In Fig. 2, we compare the energies at two momenta 0 and k_F from both the V-2ph and V-1ph methods. One can see that under V-2ph, the critical point for the transition is at $(1/k_F a_s)_c = 0.91$, very close to the critical point obtained from Monte Carlo [14] and diagrammatic [15] methods. Clearly, this critical point shifts to the weaker-coupling side as compared to the value $(1/k_F a_s)_c = 1.27$ from the V-1ph method [15–17,37]. Near the transitions, the molecule states [$M_4(0)$ under V-2ph and $M_2(0)$ under V-1ph] can well approximate the $Q = k_F$ states, and thus the transition between $Q = 0$ and $Q = k_F$ states can indeed be interpreted as the polaron-molecule transition. This sets the nature of such a first-order transition between polaron and molecule.

In Fig. 5, we further show the residue $Z = |\psi_0|^2$ as a function of $1/(k_F a_s)$ for different momentum ($Q = |\mathbf{Q}|$) states. For zero-momentum $Q = 0$, we can see that Z is insensitive to the variational approach used (V-1ph or V-2ph). However, for momentum $Q = k_F$, Z can change a lot between the V-1ph and V-2ph methods, or between $P_3(k_F)$ and $P_5(k_F)$. Moreover, for a given coupling strength, Z can be greatly reduced by increasing the momentum Q. In particular, as Q approaches k_F, the reduction of Z is quite substantial in the weak-coupling limit, implying the failure of the quasiparticle picture for the $Q \sim k_F$ state in this regime.

In the following, we comment on the nature of the polaron-molecule transition as the momentum shifts by k_F, and its implication on the huge ground-state degeneracy in the molecule limit. In Fig. 1, we show schematically the ground state switch from polaron ($\mathbf{Q} = \mathbf{0}$) to molecule ($|\mathbf{Q}| = k_F$) as the attraction between impurity ($\downarrow$) and majority fermions ($\uparrow$) increases. In the extremely weak attraction limit, it is natural to expect that the ground state is a zero-momentum polaron ($\mathbf{Q} = \mathbf{0}$) described by a zero-momentum impurity dressed with ph excitations in the majority Fermi sea. On the contrary, in the extremely strong attraction limit, the ground state is

composed by a zero-momentum molecule on top of the rest of the Fermi sea. To accomplish this, the impurity has to acquire a finite momentum $\mathbf{Q}$ such that it can pair with a fermion at the Fermi surface ($\mathbf{k}_F$) to form a zero-momentum molecule ($\mathbf{Q}+\mathbf{k}_F=\mathbf{0}$). As $\mathbf{k}_F$ can point to any direction on the Fermi surface, the direction of $\mathbf{Q}$ is also free and the system has a huge ground-state degeneracy [SO(3) for the 3D case] in this limit.

In fact, the huge SO(3) degeneracy can also be seen clearly from the molecule dispersion (32), where the energy minimum is located at a sphere in momentum space with radius $|\mathbf{Q}|=k_F$. Such a huge degeneracy in k-space resembles the single-particle SO(3) degeneracy under an isotropic spin-orbit coupling [43,44], where the ground state is located at a sphere with radius determined by the strength of spin-orbit coupling. In comparison, here the degeneracy is supported by the presence of a majority Fermi sea. An important consequence of such degeneracy is that it greatly enhances the density of states (DOS) at low-energy space near $|\mathbf{Q}|\sim k_F$, thereby significantly favoring the molecule occupation in a realistic system with a finite impurity density, as we will discuss in a later section.

Given the molecule degeneracy at momentum $|\mathbf{Q}|=k_F$, one may raise the follow question: if we equally superpose two of the $\mathbf{Q}$-states, such as $|k_F\mathbf{e}_z\rangle+|-k_F\mathbf{e}_z\rangle$, which have the same zero-averaged momentum as the polaron state, will there still be a polaron-molecule transition? The answer to this question is *yes*. This is because such a superposed state has zero overlap with the $\mathbf{Q}=\mathbf{0}$ polaron state, and thus the energy crossing between them (featuring the first-order transition) persists in changing the coupling strength. Moreover, the huge degeneracy in the molecule side will not be affected since one can in principle superpose any two momentum states $|\mathbf{Q}_1\rangle$ and $|\mathbf{Q}_2\rangle$, as long as $|\mathbf{Q}_1|=|\mathbf{Q}_2|=k_F$. In fact, such superposed state is not the eigenstate of total momentum operator $\hat{P}$. Recalling that the Hamiltonian $\hat{H}$ preserves the total momentum, i.e., $[\hat{H},\hat{P}]=0$, it is a regular strategy to look for the ground state as the eigenstate of both $\hat{H}$ and $\hat{P}$. In this sense, we recover the nature of the polaron-molecule transition as the energy competition between different $\mathbf{Q}$-sectors.

B. 2D

For a 2D Fermi polaron system, we have carried out numerical simulations using both the V-2ph and V-Gph methods and found consistent results. We use the dimensionless coupling strength $\ln(k_F a_{2d})$ to characterize the interaction effect. In our numerical calculations, we set the momentum cutoff as $k_c=30k_F$ in the V-2ph method. In the V-Gph method, we discretize the whole space to 40×40 cells, and we set the number of majority fermions as $N=49$ and the momentum cutoff as $k_c=8k_F$.

In Fig. 6, we show the energies of $P_5(k_F)$, $P_5(0)$, and $M_4(0)$ as functions of $\ln(k_F a_{2d})$, in comparison with the energies of $P_3(k_F)$, $P_3(0)$, and $M_2(0)$. One can see that similar to the 3D case, the molecule state $M_4(0)$ always has a higher energy than $P_5(\mathbf{k}_F)$; however, in the strong-coupling regime, $\ln(k_F a_{2d})<-0.7$, the two states are indistinguishable in energy, indicating that the former can serve as a good approximation for the latter. Moreover, we note from Fig. 6 that the V-2ph

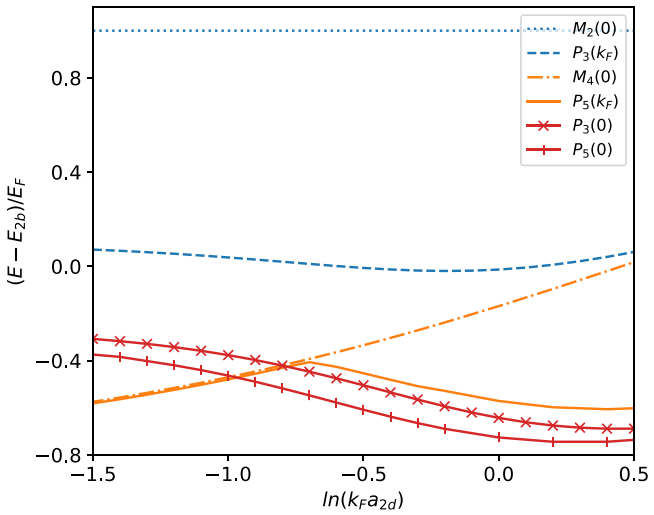

FIG. 6. Energy comparison in 2D. All energies are shifted by $E_{2b}=-1/(ma_{2d}^2)$ in order to highlight the difference.

method can produce visibly lower energy for both polaron and molecule states than V-1ph. For instance, within one ph framework, $P_3(0)$ always has a lower energy than $P_3(k_F)$ and $M_2(0)$. However, by adding two ph excitations, the molecule energy can be significantly reduced. In the strong-coupling limit, $\ln(k_F a_{2d})\to-\infty$, the energies of $P_5(k_F)$ and $M_4(0)$ (from V-2ph) both approach $E_{2b}-E_F$, much lower than the asymptotic energy $E_{2b}+E_F$ of $P_3(k_F)$ and $M_2(0)$ states (from V-1ph) in this limit. This shows a significant role played by ph excitations in 2D. However, adding more (three and above) ph excitations is not expected to lower the energy too much in the strong-coupling regime, since $E_{2b}-E_F$ sets the lower bound of the energy. This is further confirmed by the results from the V-Gph method (see Fig. 8), which includes the high-order ph excitations and gives a similar conclusion to that of the V-2ph method; see the discussions below.

In Figs. 7(a) and 7(b), we plot out the energy dispersions at various couplings from both V-2ph and V-Gph methods, from which we see that the results from the two methods are qualitatively consistent. Namely, as the attraction between the impurity and fermions increases, there is a first-order transition at a certain coupling strength where the ground state of the system switches from total momentum $Q=0$ to $Q=k_F$. Near the transition and beyond, the dispersion near $Q\sim k_F$ can indeed be well approximated by the molecule state $M_4(Q_M)$ near $Q_M\sim0$; see the triangular points in Fig. 7(a). To see more clearly the transition point, we show the energies at these two momenta as functions of coupling strengths in Fig. 8. The critical coupling at which the ground state switches from $Q=0$ to $Q=k_F$ is $\ln(k_F a_{2d})_c\approx-0.97$ from the V-2ph method, and -0.81 from V-Gph. In comparison, the critical coupling obtained from the comparison between $P_5(0)$ and $M_4(0)$ is $\ln(k_F a_{2d})_c\approx-0.98$ [24,45].

All the above results confirm a first-order polaron-molecule transition in a 2D single impurity system, and the nature of such a transition shares the same spirit as the 3D case, i.e., the energy competition between different total momenta states $\mathbf{Q}=\mathbf{0}$ and $|\mathbf{Q}|=k_F$. Since $\mathbf{Q}$ can point to any

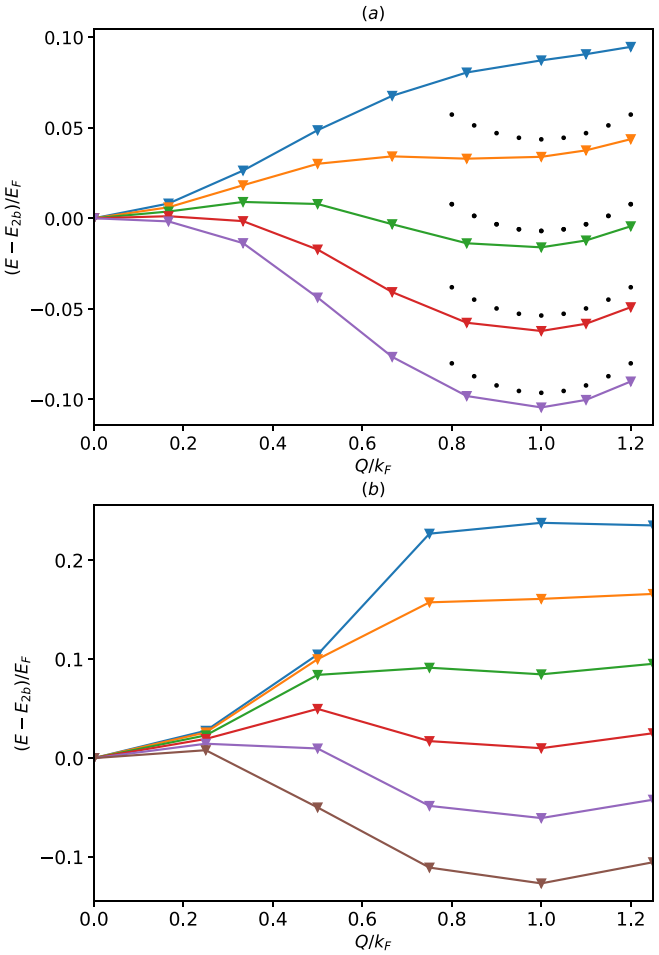

FIG. 7. (a) Energy dispersion of $P_5(\mathbf{Q})$ (solid line) in 2D at various couplings (from top to bottom) $\ln(k_F a_{2d}) = -0.8, -0.9, -1.0, -1.1, -1.2$, shifted by the values at $\mathbf{Q} = \mathbf{0}$. The small black dots show the energies from $M_4(\mathbf{Q}_M)$, with $|\mathbf{Q}_M|$ shifted by k_F in order to compare with the energies of $P_5(\mathbf{Q})$. (b) Energy dispersion from the V-Gph method at various couplings (from top to bottom) $\ln(k_F a_{2d}) = -0.5, -0.6, -0.7, -0.8, -0.9, -1.0$, again shifted by the values at $\mathbf{Q} = \mathbf{0}$. Here $Q = |\mathbf{Q}|$.

direction in the 2D plane, there will be a SO(2) ground-state degeneracy in the molecule regime with a fixed $|\mathbf{Q}| = k_F$.

We note that the polaron-molecule competition in 2D has also been investigated by Monte Carlo methods [25–27]. Among these studies, Refs. [25,26] have claimed a transition while Ref. [27] has claimed a smooth crossover between polaron and molecule. However, we note that in Ref. [27] the number of majority fermions used in the weak-coupling regime is different (by one) from that in the strong-coupling regime. This automatically changes the total momentum of the system by k_F and thus the conclusion of a smooth crossover is *not* for the same system with a fixed total momentum. Moreover, Fig. 8 shows that the shifted energy $E(k_F) - E_{2b}$ evolves nonmonotonically with $\ln(k_F a_{2d})$, different from the 3D case (see Fig. 2). In particular, in the weak-coupling regime it shares a similar functional line shape to $E(0) - E_{2b}$, which may also cause the confusion that the polaron-molecule conversion in 2D is a smooth crossover.

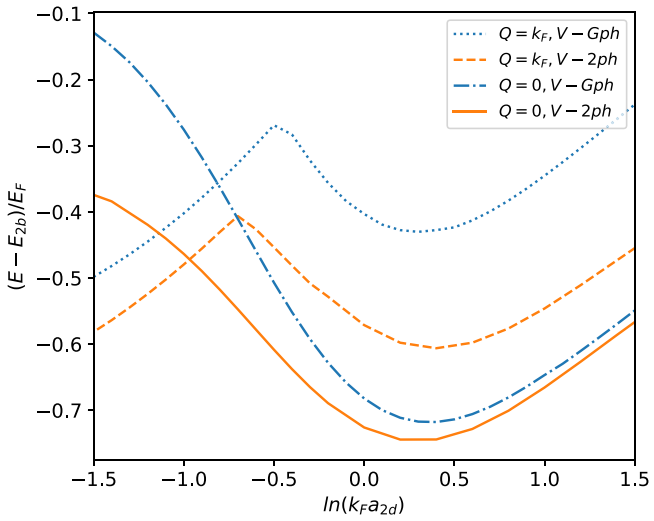

FIG. 8. Energies of $Q = 0$ and $Q = k_F$ states as functions of coupling strengths in 2D, obtained from both the V-2ph and V-Gph methods. All energies are shifted by $E_{2b} = -1/(ma_{2d}^2)$ in order to highlight the difference.

C. 1D

We will briefly go through the 1D case, where the coupling strength is governed by a dimensionless parameter $k_F a_{1d}$, with $a_{1d} = -2/(mg)$ the 1D scattering length. In our numerical calculations, we are able to compute with a different momentum cutoff k_c and finally obtain the results for $k_c \to \infty$ by extrapolation.

In Fig. 9, we show the energy dispersion at weak and strong couplings from the V-2ph method (solid lines), in comparison with those from the exact Bethe-*Ansatz* solutions [46–48] (dashed lines). It is found that the two methods give consistent conclusions that there is no transition in the system and the ground state is always at zero momentum $Q = 0$, contrary to 2D and 3D. Remarkably, the energy from the V-2ph method fits the exact solution remarkably well in the weak-coupling limit; see Fig. 9(a). For strong coupling [see Fig. 9(b)], the deviation between the two energies is attributed to the insufficiency of the V-2ph method and thus more ph excitations are required. In the strong-coupling limit, the ground-state energy (at $Q = 0$) is given by $E \to E_{2b} - E_F$, signifying a smooth crossover to the molecule regime for the 1D single-impurity system.

D. Discussion

In the above we have shown that the presence of a polaron-molecule transition depends sensitively on the dimension of the system, namely, there is such a transition in 3D and 2D but not in 1D. In the following, we point out some intrinsic reasons for this sensitive dependence on dimensionality.

Let us start from the weak-coupling regime that can be smoothly connected to the noninteracting limit. In this regime, one can easily anticipate that the ground state should be the $Q = 0$ polaron, describing a zero-momentum impurity dressed with a limited number of ph excitations of background fermions. Therefore, the key question is to find out the ground state in the strong-coupling regime, which determines whether

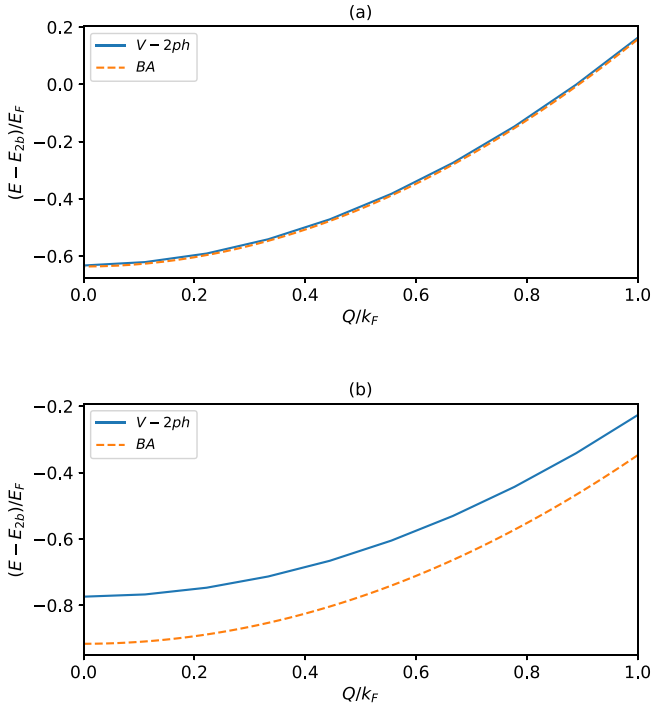

FIG. 9. Dispersion for the 1D system at different couplings $k_F a_{1d} = 1$ (a) and 0.2 (b). The solid and dashed line are, respectively, from the V-2ph and Bethe-*Ansatz* [46–48] methods, which show consistently that the ground state always stays at zero momentum. All energies are shifted by the two-body binding energy $E_{2b} = -1/(ma_{1d}^2)$.

there is a transition (switch of ground state) as the attraction is increased from weak to strong. Since the molecule state (belonging to the $Q = k_F$ sector) is an important candidate for the ground state in the strong-coupling regime, in the following we will analyze how its energy depends on the dimension. In particular, we will highlight the roles played by the Pauli-blocking effect and the ph excitations of background fermions in different dimensions.

Let us consider the bare molecule $M_2(0)$ and analyze the Pauli-blocking effect on the molecule energy. For a d-dimensional system, it has been shown that in the strong-coupling or deep molecule regime (when $|E_{2b}| \to \infty$), the molecule energy (with respect to the energy of $|\mathrm{FS}\rangle_N$) is [22]

$$E_M = E_{2b} - E_F + c_d E_F (2E_F/|E_{2b}|)^{(d-2)/2}, \qquad (33)$$

where c_d is a positive constant. One can see that in the deep molecule regime, the shift of E_M from $E_{2b} - E_F$ is negligible for 3D, a constant ($\propto E_F$) for 2D, and an exceedingly large number for 1D. It means that the effect of Pauli blocking by the underlying Fermi sea is very little for 3D molecule, but it becomes more and more significant if we go to lower dimensions. This is because in 3D, the phase space blocked by the Fermi sea is negligible as compared to the full phase space, while in lower dimensions the difference between the two phase spaces is not that substantial. As a result, the molecule becomes energetically less favored in lower dimensions systems, which may serve as a crucial reason for the absence of a polaron-molecule transition in 1D.

Moreover, we note that the ph excitations also become more and more important to affect the molecule energy than going to lower-d systems. As one can see from the energy comparison between $M_2(0)$ and $M_4(0)$ in Figs. 2 and 6, adding one more ph excitation will reduce the molecule energy by a small proportion of E_F in 3D, but by a visible constant (as large as $\sim 2E_F$) in 2D. Within V-2ph, the molecule energy in 3D and 2D in the strong-coupling regime approaches $E_{2b} - E_F$ (with respect to the energy of $|\mathrm{FS}\rangle_N$), which is the lowest energy one can imagine for the system. Therefore, there must be a transition between polaron ($Q = 0$) and molecule ($Q = k_F$) at a certain intermediate coupling strength for 3D and 2D. On the contrary, for a 1D system, the ground state is always at $Q = 0$ (see Fig. 9), and in the strong-coupling regime the energy at $Q = 0$ approaches $E_{2b} - E_F$ while at $Q = k_F$ it approaches $E_{2b} - E_F/2$. It means that in 1D, the polaron-to-molecule conversion is completed entirely within the zero-momentum sector, and thus the process is a smooth crossover rather than a transition.

The above analysis shows that it is important to consider the effects of Pauli-blocking and ph excitations in lower dimensional Fermi polaron systems. The interplay of these effects significantly influences the presence or absence of polaron-molecule transitions in different dimensions.

IV. POLARON-MOLECULE COEXISTENCE AND SMOOTH CROSSOVER IN REALISTIC FERMI POLARON SYSTEMS

In our previous work [37], we used the single-impurity result from the V-1ph method to qualitatively explain the polaron-molecule coexistence and smooth crossover as observed in recent 3D Fermi polaron systems with a finite impurity density and at finite temperature [9]. Recently, a theoretical study [49] extended the finite-momentum V-1ph method to finite-temperature and explained the smooth crossover between polaron and molecule. Here we will refine the explanation by utilizing the results from V-2ph and incorporating the trap effect through the local density approximation (LDA). In our calculation, we will take the same temperature ($T = 0.2T_F$) and the same impurity concentration as was used in the experiment in Ref. [9].

As seen from Fig. 4, the double minima structure of the single-impurity dispersion provides a clear picture of polaron-molecule coexistence under a finite impurity density and at finite temperature. As in Ref. [37], we will neglect the thermal distortion of majority Fermi sea and mediated interactions between the impurities (including polaron-polaron, polaron-molecule, and molecule-molecule interactions), which are expected to produce invisible effects at sufficiently low impurity densities. Here we only focus on two possible configurations for the dressed impurities: one is "polaron" near zero-momentum and obeying fermionic statistics; the other is "molecule" near $|\mathbf{Q}| = k_F$ and obeying bosonic statistics.

Now we discuss how to separate the polaron and molecule in the dispersion curve. In the polaron-molecule coexistence regime $1/(k_F a_s) \in (0.5, 1.2)$, there is a natural momentum boundary in the diversion curve, denoted as Q_c, that can be chosen as the location of the energy maximum between $Q = 0$ and $Q = k_F$, as marked by squares in Fig. 4. After defining Q_c, the energy cutoff for the thermal excitation of impurities is also fixed as $E_c = E(Q_c)$. More specifically, the polaron

occupies at $|\mathbf{Q}| < Q_c$ and the molecule occupies at $|\mathbf{Q}| > Q_c$ with energy cutoff E_c. The value of Q_c outside the coexistence regime is defined as follows. In the weak-coupling regime, $1/(k_F a_s) < 0.5$, the impurities occupy as polarons and there is no molecule distribution; in this case, we define Q_c as the polaron momentum when its residue reduces to 0.01. In the strong-coupling regime, $1/(k_F a_s) > 1.2$, the polaron vanishes and all impurities occupy as molecules; in this case, we simply take $Q_c = 0$.

Next we incorporate the trap effect. For the majority fermions, we use the zero-temperature density distribution as the approximation:

$$n_\uparrow(\mathbf{r}) = \frac{1}{6\pi^2}\{2m[\mu_\uparrow - V(\mathbf{r})]\}^{\frac{3}{2}}, \tag{34}$$

where $V(\mathbf{r}) = m\omega^2\mathbf{r}^2/2$ is the trap potential and $\mu_\uparrow = k_{F\uparrow}^2(0)/(2m) = (6N_\uparrow)^{1/3}\omega$ is the chemical potential of majority fermions at the center of the trap. Under LDA, one can define the local Fermi momentum as $k_{F\uparrow}(\mathbf{r}) = [6\pi^2 n_\uparrow(\mathbf{r})]^{1/3}$, which determines the local occupation of polaron and molecule states.

Under the above assumptions, the local impurity density can be written as [with a $\theta(x)$ step function]

$$\begin{aligned} n_\downarrow(\mathbf{r}) = \int \frac{d^3\mathbf{Q}}{(2\pi)^3}[&n_F(E(\mathbf{Q},\mathbf{r}),\mu_\downarrow,V_\downarrow(\mathbf{r}))\,\theta(Q_c - |\mathbf{Q}|) \\ &+ n_B(E(\mathbf{Q},\mathbf{r}),\mu_\downarrow,V_\downarrow(r))\,\theta(|\mathbf{Q}| - Q_c) \\ &\times \theta(E_c - E(\mathbf{Q},\mathbf{r}))], \end{aligned} \tag{35}$$

where $n_{F/B}(E,\mu_\downarrow,V_\downarrow(\mathbf{r})) = [1 \pm \exp(\frac{E-\mu_\downarrow+V_\downarrow(\mathbf{r})}{k_B T})]^{-1}$, and $V_\downarrow(\mathbf{r}) = V_\uparrow(\mathbf{r})(1 - \frac{E}{E_F})$ is the renormalized trap potential felt by impurity atoms [9,11]. Note that because of the $\mathbf{r}$-dependence of local $k_{F\uparrow}$, the quantities E, Q_c, and E_c in the above equation all depend locally on $\mathbf{r}$.

Following the definition of the averaged density ratio in [9],

$$\left\langle \frac{n_\downarrow}{n_\uparrow} \right\rangle = \frac{\int d^3\mathbf{r} n_\downarrow(\mathbf{r}) \frac{n_\downarrow(\mathbf{r})}{n_\uparrow(\mathbf{r})}}{\int d^3\mathbf{r} n_\downarrow(\mathbf{r})}, \tag{36}$$

in our calculation we will set $\langle \frac{n_\downarrow}{n_\uparrow} \rangle = 0.15$ as in Ref. [9], which is used to determine $\mu_\downarrow$ in Eq. (35). Then we go further to calculate the trap-averaged residue, the contact, and the polaron energy by

$$\begin{aligned} \bar{Z} &= \frac{\int d^3\mathbf{r} n_\downarrow(\mathbf{r}) Z(\mathbf{r})}{\int d^3 r n_\downarrow(\mathbf{r})}, \\ \bar{C} &= \frac{\int d^3\mathbf{r} n_\downarrow(\mathbf{r}) C(\mathbf{r})}{\int d^3 r n_\downarrow(\mathbf{r})}, \\ \bar{E}_{\rm pol} &= \frac{\int d^3\mathbf{r} n_\downarrow(\mathbf{r}) E_{\rm pol}(\mathbf{r})}{\int d^3\mathbf{r} n_\downarrow(\mathbf{r})}, \end{aligned} \tag{37}$$

where $Z(\mathbf{r})$, $C(\mathbf{r})$, and $E_{\rm pol}(\mathbf{r})$ are

$$\begin{aligned} Z(\mathbf{r}) &= \frac{1}{n_\downarrow(\mathbf{r})} \int \frac{d^3\mathbf{k}}{(2\pi)^3} Z(\mathbf{k}) n_F(E(\mathbf{k},\mathbf{r}),\mu_\downarrow,V_\downarrow(\mathbf{r}))\theta(Q_c - |\mathbf{k}|), \\ C(\mathbf{r}) &= \frac{4\pi m}{2n_\downarrow(\mathbf{r})k_F^2} \int \frac{d^3\mathbf{k}}{(2\pi)^3} \frac{dE(\mathbf{k},\mathbf{r})}{d(1/k_F a_s)} n_F(E(\mathbf{k},\mathbf{r}),\mu_\downarrow,V_\downarrow(\mathbf{r}))\theta(Q_c - |\mathbf{k}|) \\ &\quad + \frac{4\pi m}{2n_\downarrow(\mathbf{r})k_F^2} \int \frac{d^3\mathbf{k}}{(2\pi)^3} \frac{dE(\mathbf{k},\mathbf{r})}{d(1/k_F a_s)} n_B(E(\mathbf{k},\mathbf{r}),\mu_\downarrow,V_\downarrow(\mathbf{r}))\,\theta(|\mathbf{k}| - Q_c)\,\theta(E_c - E(\mathbf{k},\mathbf{r})), \\ E_{\rm pol}(\mathbf{r}) &= E(k = 0, \mathbf{r}). \end{aligned} \tag{38}$$

In Figs. 10(a)–10(c), we show the calculated $\bar{Z}$, $\bar{C}$, and $\bar{E}_p$ (see orange circles and lines) as functions of coupling strength, in comparison with the experimental data in Ref. [9] (shown as blue circles with error bars) and the theory prediction therein based on the separate treatment of polaron (under V-1ph) and molecule (no ph excitation) while without considering the SO(3) degeneracy of molecules (shown by black dashed-dot lines). We can see that compared to the theory prediction in Ref. [9], our prediction of $\bar{Z}$ is visibly lower and the prediction of $\bar{C}$ is visibly higher, giving a better fit to the experimental data in the weak-coupling and near-resonance regime. These visible improvements can be attributed to the following two reasons:

First, compared to the V-1ph method, the inclusion of two ph excitations in V-2ph does not change too much the polaron energy but reduces the molecule energy considerably; see Fig. 2. A direct consequence of this change is to move the polaron-molecule transition point and their coexistence region to the weaker coupling side. The other consequence is to enhance the molecule occupation in the coexistence regime. These two factors both contribute to reducing the residue $\bar{Z}$ and increasing the contact $\bar{C}$ for a given coupling strength.

Secondly, we have a different classification and sampling scheme for the polaron and molecule as compared to Ref. [9]. In particular, in the theory of Ref. [9] the molecule dispersion is centered at zero rather than k_F, and thus the SO(3) degeneracy is not considered. This significantly underestimates the molecule occupation number due to the small density of states (DOS) near $\mathbf{Q} \sim \mathbf{0}$. In comparison, in this work we point out that the molecule actually stays around $|\mathbf{Q}| \sim k_F$ with a huge SO(3) degeneracy and thus a much larger DOS at low energy. This will also help to enhance the molecule occupation further and lead to a smaller $\bar{Z}$ and a larger $\bar{C}$ than the theory prediction in Ref. [9].

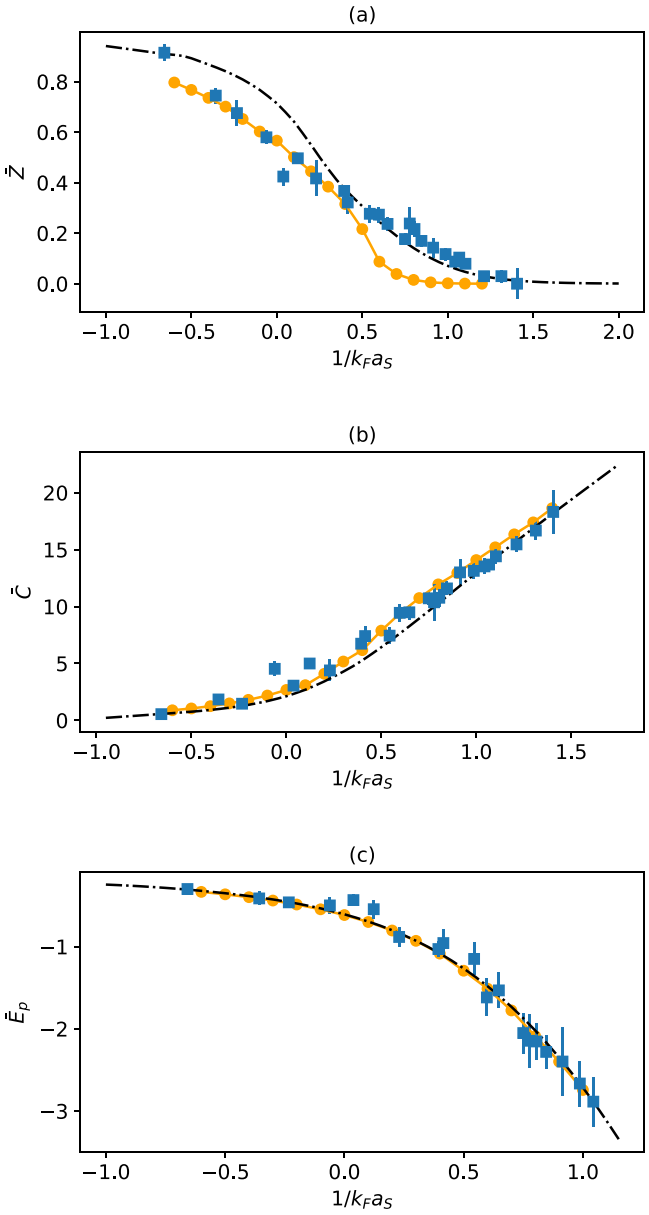

FIG. 10. Residue $\bar{Z}$ (a), contact $\bar{C}$ (b), and the polaron energy $\bar{E}_p$ (c) as functions of coupling strength given the realistic experimental condition in Ref. [9]. The blue squares with an error bar show the experimental results in Ref. [9]. Black dashed-dot lines show the theoretical prediction in Ref. [9] based on the separate treatment of polaron (under V-1ph) and molecule (no ph excitation) without considering the SO(3) degeneracy. Orange circles and lines show our results based on V-2ph plus LDA. Here k_F is the Fermi momentum of majority fermions at the trap center.

To examine the individual contributions of the above two effects, in Fig. 11 we plot $\bar{Z}$ as a function of coupling strength from the combination of different methods (V-1ph or V-2ph) and different sampling schemes [with or without considering SO(3) degeneracy of molecules]. We can see that in the weak-coupling regime, $\bar{Z}$ can be visibly reduced by including two ph excitations, which can be attributed to the sensitive change of Z for the finite-momentum polaron (note that the residue of the $\mathbf{Q} = \mathbf{0}$ polaron shows little difference between V-1ph and

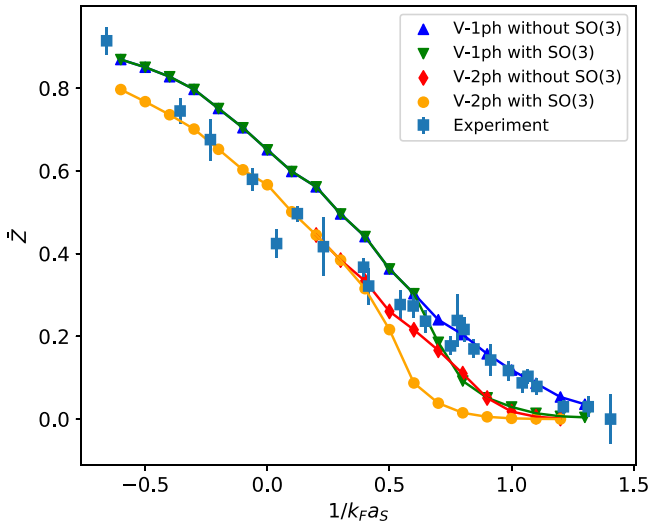

FIG. 11. Residue $\bar{Z}$ from the combination of different methods (V-1ph or V-2ph) and different sampling schemes [with or without considering SO(3) degeneracy of molecules]. The blue squares with an error bar show the experimental results of Ref. [9].

V-2ph methods; see Fig. 5). In this regime, the SO(3) degeneracy has no effect since there is no molecule occupation yet. However, when going to the strong-coupling regime where the polaron and molecule coexist, the SO(3) degeneracy plays an important role in enhancing the molecule occupation and reducing $\bar{Z}$, regardless of the order of ph excitations.

Finally, it is noted that our theory does not fit well to the experimental data of $\bar{Z}$ in the strong-coupling regime. For instance, $\bar{Z}$ from our prediction continuously drops to zero around $1/(k_F a_s) \sim 0.9$, very close to the polaron-molecule transition point ($\sim$0.91) for the single-impurity system. Nevertheless, the data of $\bar{Z}$ in Ref. [9] show a long tail in this regime and seem to be better fit by V-1ph results without considering the SO(3) degeneracy of molecules. Possible reasons for the discrepancy are as follows. First, the data of $\bar{Z}$ in Ref. [9] are not from a direct measurement; instead, they are extracted from the total Raman spectrum of impurities that is parametrized by six free parameters ($\bar{Z}$ is one of them). Moreover, the parametrization of the background Raman signal therein is based on the assumption of thermal occupation of a bare molecule without SO(3) degeneracy. All of these assumptions may cause the deviation of $\bar{Z}$ from its actual value, especially in the polaron-molecule coexistence regime. Thus, the deterministic test of different theories calls for future experimentation with a more accurate and direct probe of various physical quantities.

V. SUMMARY

In this work, we have investigated the polaron and molecule physics in 3D, 2D, and 1D Fermi polaron systems by utilizing a unified variational *Ansatz* with up to two ph excitations (V-2ph). Moreover, we have checked the reliability of our results by comparing with the result from the variational method in 2D based on the Gaussian sample of high-order ph excitations (V-Gph), and with the result of Bethe-*Ansatz*

solutions in 1D. These methods produce consistent conclusions, which are summarized as follows:

(i) There exists a first-order transition for a single-impurity system in 3D and 2D as the attraction between the impurity and fermions increases. The nature of such a transition lies in an energy competition between different total momenta $\mathbf{Q} = \mathbf{0}$ and $|\mathbf{Q}| = k_F$, with k_F the Fermi momentum of majority fermions. From the V-2ph method, the transition point is at $1/(k_F a_s) = 0.91$ for 3D and at $\ln(k_F a_{2d}) = -0.97$ for 2D. In 1D, there is no transition and the ground state is always at $Q = 0$ for all couplings. The underlying reason for the presence/absence of such a transition is analyzed to be closely related to the interplay effect of Pauli-blocking and ph excitations in different dimensions.

(ii) The literally proposed molecule state has an incomplete variational space in terms of ph excitations, but it can serve as a good approximation for the $Q = k_F$ state in the strong-coupling regime. Due to the finite momentum, the ground state in the molecule regime has a huge degeneracy [SO(3) for 3D and SO(2) for 2D], which can greatly enhance the low-energy density of states for the molecule occupation in realistic Fermi polaron systems with a finite impurity density. Our theory explains well the coexistence and a smooth crossover between polaron and molecule as observed in a recent 3D Fermi polaron experiment [9], and it also produces quantitatively good fits to various physical quantities measured in the weak-coupling and resonance regime of the system.

In the future, it would be interesting to extend our theory to various other impurity systems, such as with different mass ratios between the impurity and the background, as well as the regime with strong three-body correlations where the trimer physics can dominate.

ACKNOWLEDGMENTS

We thank Yoav Sagi for sharing with us the data in the experiment from Ref. [9]. This work is supported by the National Key Research and Development Program of China (2018YFA0307600, 2016YFA0300603), the National Natural Science Foundation of China (11774425, 12074419), and the Strategic Priority Research Program of Chinese Academy of Sciences (XDB33000000).

[1] L. D. Landau, Phys. Z. Sowjetunion **3**, 664 (1933).
[2] A. Schirotzek, C.-H. Wu, A. Sommer, and M. W. Zwierlein, Phys. Rev. Lett. **102**, 230402 (2009).
[3] S. Nascimbéne, N. Navon, K. J. Jiang, L. Tarruell, M. Teichmann, J. McKeever, F. Chevy, and C. Salomon, Phys. Rev. Lett. **103**, 170402 (2009).
[4] N. Navon, S. Nascimbéne, F. Chevy, and C. Salomon, Science **328**, 729 (2010).
[5] C. Kohstall, M. Zaccanti, M. Jag, A. Trenkwalder, P. Massignan, G. M. Bruun, F. Schreck, and R. Grimm, Nature **485**, 615 (2012).
[6] M. Koschorreck, D. Pertot, E. Vogt, B. Frölich, M. Feld, and M. Köhl, Nature (London) **485**, 619 (2012).
[7] M. Cetina, M. Jag, R. S. Lous, I. Fritsche, J. T. M. Walraven, R. Grimm, J. Levinsen, M. M. Parish, R. Schmidt, M. Knap, and E. Demler, Science **354**, 96 (2016).
[8] F. Scazza, G. Valtolina, P. Massignan, A. Recati, A. Amico, A. Burchianti, C. Fort, M. Inguscio, M. Zaccanti, and G. Roati, Phys. Rev. Lett. **118**, 083602 (2017).
[9] G. Ness, C. Shkedrov, Y. Florshaim, O. K. Diessel, J. von Milczewski, R. Schmidt, and Y. Sagi, Phys. Rev. X **10**, 041019 (2020).
[10] F. Chevy, Phys. Rev. A **74**, 063628 (2006).
[11] C. Lobo, A. Recati, S. Giorgini, and S. Stringari, Phys. Rev. Lett. **97**, 200403 (2006).
[12] R. Combescot, A. Recati, C. Lobo, and F. Chevy, Phys. Rev. Lett. **98**, 180402 (2007).
[13] R. Combescot and S. Giraud, Phys. Rev. Lett. **101**, 050404 (2008).
[14] N. V. Prokof'ev and B. V. Svistunov, Phys. Rev. B **77**, 125101 (2008); **77**, 020408(R) (2008).
[15] R. Combescot, S. Giraud, and X. Leyronas, Europhys. Lett. **88**, 60007 (2009).
[16] M. Punk, P. T. Dumitrescu, and W. Zwerger, Phys. Rev. A **80**, 053605 (2009).
[17] C. Mora and F. Chevy, Phys. Rev. A **80**, 033607 (2009).
[18] G. M. Bruun and P. Massignan, Phys. Rev. Lett. **105**, 020403 (2010).
[19] R. Schmidt and T. Enss, Phys. Rev. A **83**, 063620 (2011).
[20] C. Trefzger and Y. Castin, Phys. Rev. A **85**, 053612 (2012).
[21] C. J. M. Mathy, M. M. Parish, and D. A. Huse, Phys. Rev. Lett. **106**, 166404 (2011).
[22] S. Zollner, G. M. Bruun, and C. J. Pethick, Phys. Rev. A **83**, 021603(R) (2011).
[23] M. M. Parish, Phys. Rev. A **83**, 051603(R) (2011).
[24] M. M. Parish and J. Levinsen, Phys. Rev. A **87**, 033616 (2013).
[25] J. Vlietinck, J. Ryckebusch, and K. Van Houcke, Phys. Rev. B **89**, 085119 (2014).
[26] P. Kroiss and L. Pollet, Phys. Rev. B **90**, 104510 (2014).
[27] S. Bour, D. Lee, H.-W. Hammer, and U.-G. Meißner, Phys. Rev. Lett. **115**, 185301 (2015).
[28] R. Liu, Y.-R. Shi, and W. Zhang, Phys. Rev. A **102**, 033305 (2020).
[29] S. Giraud and R. Combescot, Phys. Rev. A **79**, 043615 (2009).
[30] J.-G. Chen, T.-S. Deng, W. Yi, and W. Zhang, Phys. Rev. A **94**, 053627 (2016).
[31] X. Cui and H. Zhai, Phys. Rev. A **81**, 041602(R) (2010).
[32] S. Pilati, G. Bertaina, S. Giorgini, and M. Troyer, Phys. Rev. Lett. **105**, 030405 (2010).
[33] P. Massignan and G. M. Bruun, Eur. Phys. J. D **65**, 83 (2011).
[34] V. Ngampruetikorn, J. Levinsen, and M. M. Parish, Europhys. Lett. **98**, 30005 (2012).
[35] R. Schmidt, T. Enss, V. Pietila, and E. Demler, Phys. Rev. A **85**, 021602(R) (2012).
[36] D. M. Edwards, J. Phys.: Condens. Matter **25**, 425602 (2013).
[37] X. Cui, Phys. Rev. A **102**, 061301(R) (2020).
[38] T. Shi, E. Demler, and J. I. Cirac, Ann. Phys. **390**, 245 (2018).
[39] S. Bravyi and D. Gosset, Commun. Math. Phys. **356**, 451 (2017).

[40] C. V. Kraus, M. M. Wolf, J. I. Cirac, and G. Giedke, Phys. Rev. A **79**, 012306 (2009).
[41] T. D. Lee, F. E. Low, and D. Pines, Phys. Rev. **90**, 297 (1953).
[42] P. E. Dolgirev, Y. F. Qu, M. B. Zvonarev, T. Shi, and E. Demler, arXiv:2008.02416.
[43] J. P. Vyasanakere and V. B. Shenoy, Phys. Rev. B **83**, 094515 (2011).
[44] X. Cui, Phys. Rev. A **85**, 022705 (2012).
[45] We note that Ref. [24] obtained the transition point between $P_5(0)$ and $M_4(0)$ as $\ln(k_F a_{2d})_c = -0.97$. The slight difference between this result and ours is due to numerical errors.
[46] J. B. McGuire, J. Math. Phys. **7**, 123 (1966).
[47] X. Guan, Front. Phys. **7**, 8 (2012).
[48] O. Gamayun, O. Lychkovskiy, and M. B. Zvonarev, SciPost Phys. **8**, 53 (2020).
[49] M. M. Parish, H. S. Adlong, W. E. Liu, and J. Levinsen, Phys. Rev. A **103**, 023312 (2021).